PASSIVE CONTROL OF AIRFOIL FLUTTER USING A NONLINEAR TUNED VIBRATION ABSORBER

Arnaud Malher, Cyril Touzé, Olivier Doaré, Giuseppe Habib, Gaëtan Kerschen

PASSIVE CONTROL OF AIRFOIL FLUTTER USING A NONLINEAR TUNED VIBRATION ABSORBER

Arnaud Malher*
Cyril Touzé
Olivier Doaré
IMSIA
ENSTA ParisTech - CNRS - EDF - CEA
Université Paris-Saclay
828 Bd des Marchaux
91732 Palaiseau Cedex
Email: arnaud.malher@ensta-paristech.fr

Giuseppe HABIB
Gaëtan KERSCHEN
Space Structures and Systems Laboratory
Department of Aerospace and Mechanical Engineering
University of Liege

ABSTRACT

The influence of a Nonlinear Tuned Vibration Absorber (NLTVA) on the airfoil flutter is investigated. In particular, its effect on the instability threshold and the potential subriticality of the bifurcation is analyzed. For that purpose, the airfoil is modeled using the classical pitch and plunge aeroelastic model together with a linear approach for the aerodynamic loads. To ensure limit cycle oscillation (LCO) to the airfoil in its post-critical regime, cubic nonlinearities are added to the structural model. The influence of each NLTVA parameter is studied and an optimum tuning of these parameters is found. The study reveals the ability of the NLTVA to both shift the instability and avoid its possible subcriticality.

INTRODUCTION

When slender structures, such as bridge deck or airfoil, undergo wind excitation, the flutter instability may arise and lead to a Hopf bifurcation. The flow velocity for which the instability starts is called *flutter velocity*. This phenomenon is detrimental and may even lead to fatal vibrations of the structure. This work focuses on the flutter occurring with airfoils and a passive control strategy is proposed in order to prevent its occurrence and reduce its effects.

One of the main studies on the airfoil flutter passive control is proposed by Lee *et al.* [1, 2] and deals with the use of a nonlinear energy sink, showing promising results in the LCOs reduction. In the present study, the use of a nonlinear tuned vibration absorber (NLTVA) as proposed by Kerschen *et al* in *e.g.* [3, 4] is investigated. This absorber shares common characteristics with the tuned vibration absorbers initially developed by Den Hartog [5]. In particular, the eigenfrequency as well as the damping ratio of the absorber, which is composed of a small mass connected to the principal structure, is tuned in order to control linear vibrations [6–8]. The distinctive feature of the NLTVA is that the absorber possesses also a nonlinear stiffness, which may be tuned in order to control nonlinear vibrations of the primary structure. The influence of the NLTVA has been studied on a Van der Pol-Duffing oscillator and has shown its ability to shift the system instability threshold, reduce the LCO amplitude and cancel the potential subcriticality of the instability [9].

In the present context of the flutter instability, two main design rules are followed for optimising the NLTVA characteristics. First, the linear stiffness of the absorber is tuned in order to increase as much as possible the critical flutter velocity, thus repelling the appearance of LCO to larger flow velocities. Secondly, the nonlinear stiffness of the NLTVA may be tuned in order to enforce supercriticality, as well as to reduce the LCO amplitudes.

The airfoil is modeled using the classical pitch and plunge model [10]. The quasi-steady theory is used to estimate the aerodynamic loads. Eventually the nonlinearities, required to allow the system to develop LCO in the post-critical regime, are realized by adding cubic stiffness in the pitch and plunge motion.

The first section is devoted to the linear stability analysis. The optimisation of the linear characteristics of the vibration absorber is investigated, showing in particular how the flutter velocity can be repelled to larger values using a well-tuned absorber. In a second section, the influence of the nonlinear part of the NLTVA is investigated. In partic-

*Address all correspondence to this author.

ular, the effect of the nonlinear stiffness of the absorber is investigated in order to find the values that enforce supercriticality. These results are important and gives a number of fruitful strategies in order to better control the flutter instability by means of a nonlinear vibration absorber.

STABILITY ANALYSIS

In this section, the equations of motion are given and a tuning rule is established in order to optimize the linear part of the NLTVA.

Model equations

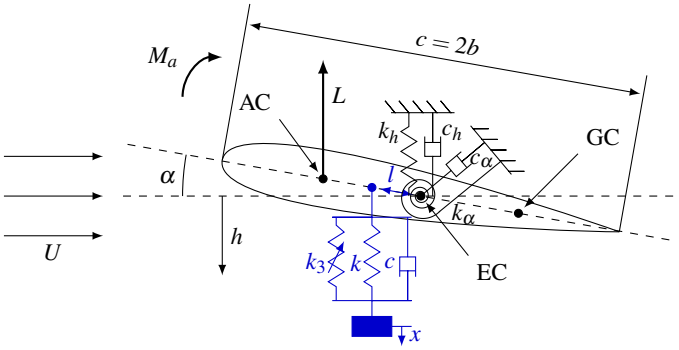

FIGURE 1: Sketch of the two degrees of freedom airfoil (main structure) coupled with the NLTVA (absorber) in blue.

The classical pitch and plunge model is used to describe the airfoil motion, see e.g. [10]. Pitch and plunge are respectively described by the heave h and the angle of attack α as shown in Fig. 1, where EC refers to the elastic center, AC to the aerodynamic center and GC to the gravity center. U is the upstream flow speed, c the chord and b the mid-chord of the plate. The distance between AC and EC is denoted by e. The NLTVA is attached along the mid-chord of the airfoil at distance l from EC. k_h, k_α and k refer to the plunge, pitch and NLTVA stiffnesses. k_3 is the cubic stiffness of the NLTVA, for the stability analysis $k_3 = 0$. c_h, c_α and c refer to the plunge, pitch and NLTVA viscous damping. The inertia moment is denoted by I_α, the airfoil mass by m and the static moment by S_α. The static moment is proportional to the distance between GC and EC and is responsible of the coupling. Eventually, L and M_a are the aerodynamic lift and moment. In the context of the quasi-steady theory they are equal to $(1/2)\rho S U^2 \mathrm{d}C_l(\alpha + \dot{h}/U)$ and $(1/2)\rho S c U^2 e\,\mathrm{d}C_l(\alpha + \dot{h}/U)$ respectively. S is the lifting surface, ρ is the fluid density and $\mathrm{d}C_l$ is the slope at zero angle of attack of L. Finally, the equations of motion read :

$$M\ddot{h} + S_\alpha\ddot{\alpha} + (c_h + BU)\dot{h} + c(\dot{h} - \dot{x} - l\dot{\alpha}) + k_h h + BU^2\alpha + k(h - x - l\alpha) = 0, \quad (1a)$$

$$I_\alpha\ddot{\alpha} + S_\alpha\ddot{h} + c_\alpha\dot{\alpha} + cl(\dot{x} + l\dot{\alpha} - \dot{h}) - NU\dot{h} + (k_\alpha - NU^2)\alpha + k(x + l\alpha - h) = 0, \quad (1b)$$

$$m\ddot{x} + c(\dot{x} - \dot{h} + l\dot{\alpha}) + k(x - h + l\alpha) = 0, \quad (1c)$$

where $B = (1/2)\rho S\,\mathrm{d}C_l$ and $N = (1/2)\rho S e\,\mathrm{d}C_l$. By introducing the following nondimensional parameters :

$$y = h/b,\ \tilde{x} = x/b,\ r_\alpha = \sqrt{I_\alpha/Mb^2},\ x_\alpha = S_\alpha/Mb,\ \lambda = l/b,$$
$$\omega_\alpha = \sqrt{k_\alpha/I_\alpha},\ \omega_h = \sqrt{k_h/M},\ \omega = \sqrt{k/m},\ \Omega = \omega_h/\omega_\alpha,$$
$$\zeta_\alpha = c_\alpha/M\omega_\alpha b^2,\ \zeta_h = c_h/M\omega_\alpha,\ \zeta = c/m\omega_\alpha,\ \tilde{U} = U/b\omega_\alpha,$$
$$\beta = B/M,\ \nu = N/M \text{ and } \tau = \omega_\alpha t,\ \varepsilon = m/M,\ \gamma = \omega^2/\omega_\alpha^2.$$

The following system is obtained :

$$\mathbf{M}\mathbf{q}'' + \mathbf{C}\mathbf{q}' + \mathbf{K}\mathbf{q} = 0, \quad (2)$$

with

$$\mathbf{q} = \begin{bmatrix} y \\ \alpha \\ \tilde{x} \end{bmatrix}, \mathbf{M} = \begin{bmatrix} 1 & x_\alpha & 0 \\ x_\alpha & r_\alpha^2 & 0 \\ 0 & 0 & 1 \end{bmatrix},$$

$$\mathbf{C} = \begin{bmatrix} \zeta_h + \varepsilon\zeta + \beta\tilde{U} & -\varepsilon\zeta\lambda & -\varepsilon\zeta \\ -\nu\tilde{U} - \varepsilon\zeta\lambda & \zeta_\alpha + \varepsilon\zeta\lambda^2 & \varepsilon\zeta\lambda \\ -\zeta & \zeta\lambda & \zeta \end{bmatrix},$$

$$\mathbf{K} = \begin{bmatrix} \Omega^2 + \varepsilon\gamma & \beta\tilde{U}^2 - \varepsilon\gamma\lambda & -\varepsilon\gamma \\ -\varepsilon\gamma\lambda & r_\alpha^2 - \nu\tilde{U}^2 + \varepsilon\gamma\lambda^2 & \varepsilon\gamma\lambda \\ -\gamma & \gamma\lambda & \gamma \end{bmatrix},$$

where $()' = d/d\tau$. The characteristics of the NLTVA are defined thanks to the following four parameters:

1. the mass ratio $\varepsilon = m/M$, between the mass of the NLTVA and that of the wing;
2. the distance l that specifies the location where the NLTVA is attached;
3. the NLTVA reduced eigenfrequency $\gamma = \omega^2/\omega_\alpha^2$, characterizing the eigenfrequency of the NLTVA compared to that of pitch motion;
4. the NLTVA damping ratio $\zeta = c/m\omega_\alpha$.

For the present study, the mass ratio has been taken equal to 5%. The larger ε the more efficient the NLTVA will be, however one must keep in mind that the absorber need to

have a negligible mass as compared to the airfoil. For this study, the NLTVA is located at the leading edge of the profile, thus $l = b$. Note that its effect is directly proportional to l, hence the location where the optimal influence on the airfoil has been selected. Eventually, γ and ζ are thus selected as our control parameters, the optimal tuning of which is searched for.
The value of the coefficients of Eq. (2) are taken from [10] and gathered in table 1.

x_α	r_α	β	ν	Ω	ζ_α	ζ_h
0.2	0.5	0.2	0.08	0.5	0.01	0.01

TABLE 1: Nondimensional aeroelastic parameters

Optimization of the NLTVA linear parameters.

In this section, the linear stability analysis is conducted. The system described by Eqs. (2) undergoes a Hopf bifurcation when $\tilde{U}$ reaches the flutter velocity $\tilde{U}_f$. Above this value, LCO arise. The aim of this section is to study the influence of our design parameters γ and ζ on the flutter velocity $\tilde{U}_f$. The targeted optimal values are those for which $\tilde{U}_f$ is as large as possible, in order to repel the instability. The stability of the system is investigated through its characteristic polynomial which reads

$$\mathscr{P}(z) = a_6 z^6 + a_5 z^5 + a_4 z^4 + a_3 z^3 + a_2 z^2 + a_1 z + a_0 = 0, \tag{3}$$

where a_1 to a_6 are detailed in Appendix A. The Routh-Hurwitz criterion is used to determine when one of the roots of $\mathscr{P}$ has a positive real part.
This study leads to four independent conditions called b_5, c_5, d_5 and e_5, which read

$$\begin{aligned} b_5 &= (a_5 a_4 - a_6 a_3)/a_5 > 0, \\ c_5 &= b_5 a_3 - a_5 b_4 > 0, \\ d_5 &= c_5 b_4 - c_4 b_5 > 0, \\ e_5 &= d_5 c_4 - d_4 c_5 > 0, \end{aligned}$$

with

$$\begin{aligned} b_4 &= (a_5 a_2 - a_6 a_1)/a_5, \\ b_3 &= a_0, \\ c_4 &= (b_5 a_3 - b_3 a_5)/b_5, \\ d_4 &= b_3. \end{aligned}$$

These four conditions are plotted as an example in Fig. 2 for $\zeta = 0.15$. Each line corresponds to the points where one of the four expressions b_5 to e_5 becomes positive, as a function of the reduced eigenfrequency γ, and for increasing values of $\tilde{U}$. Thus, the flutter velocity corresponds to the lowest curve and the stability zone to the area below it, represented as a gray-shaded area in Fig. 2. It has been remarked that in our case, the condition e_5 is always the most restrictive one and then is the only one to consider for determining $\tilde{U}_f$.

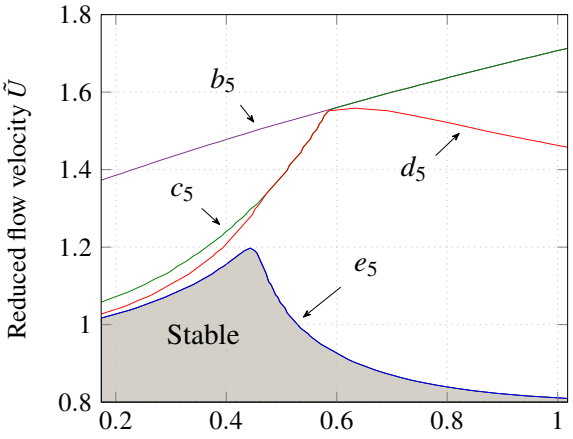

FIGURE 2: Reduced flutter velocity given by the Routh Hurwitz criterion as a function of the NLTVA reduced eigenfrequency γ, and for a damping ratio $\zeta = 0.15$. The gray area corresponds to the stability of the system.

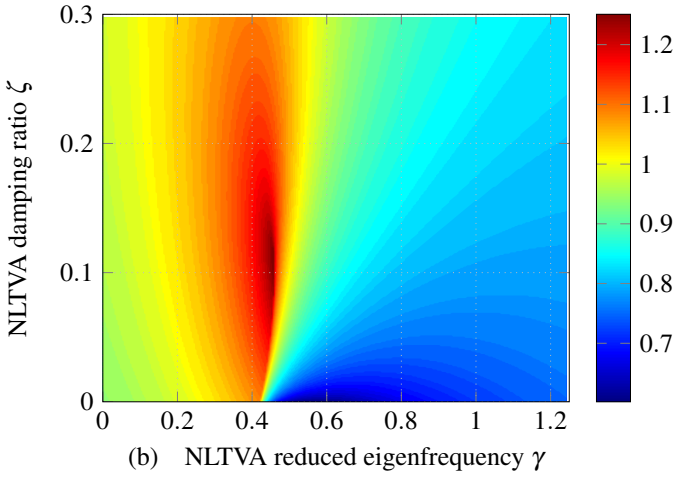

FIGURE 3: Cartography of the reduced flutter velocity given by the criterion e_5 as a function of the NLTVA reduced frequency γ and damping ratio ζ.

This calculation is then conducted for different values of ζ in order to find the optimal couple (γ_{opt},ζ_{opt}) for which the flutter velocity is maximal. The result is shown in figure 3. The maximal reduced flutter velocity, obtained for $\gamma = 0.462$ and $\zeta = 0.11$, is equal to 1.255, which means a 34.5% gain as compared to the flutter velocity without NLTVA, which is equal to 0.934. The expression of e_5 being tedious and nonlinear, an analytic expression for the optimal values of ζ and γ cannot be exhibited. Nevertheless these optimal values can be found numerically.

In practical situation, a slight detuning of γ and ζ may occur. Thus an insight on the sensitivity of $\tilde{U}_f$ regarding these parameters is interesting. It is shown in Fig. 3 that γ has more influence on $\tilde{U}_f$ than ζ. Indeed a 10% increase of γ gives a 20% decrease of $\tilde{U}_f$ and a 10% decrease of γ implies a 7% decrease of $\tilde{U}_f$, whereas a 10% increase or decrease of ζ gives a 4% decrease of $\tilde{U}_f$. Thus the optimal control should guarantee $\gamma \leq \gamma_{opt}$.

NONLINEAR ANALYSIS

This section is devoted to the tuning methodology for optimizing the nonlinear stiffness of the NLTVA. Two goals are in view. First, one would like to ensure a supercritical bifurcation, as being a more comfortable case for an engineering design with respect of the global stability of the airfoil. Second, the post-critical LCO amplitudes are investigated in order to decrease their amplitudes as much as possible.

Criticality analysis

The Hopf bifurcation encountered at $\tilde{U} = \tilde{U}_f$ can be either subcritical or supercritical. In a normal form analysis of the bifurcation, this characteristic is simply given by the sign of the cubic nonlinear term when the system is written in polar form [11–13]. The aim of this section is to obtain the expression of this coefficient, based on a reduced-order model that contains the leading order nonlinearity of the normal form. The technique used follows classical methods for dynamical systems [11, 14] that have been recently applied on a Van der Pol-Duffing oscillator [15]. The first step is to recast the equations of motion (2) as a first-order dynamical system. Nonlinear terms in the plunge and pitch stiffnesses are introduced in a similar fashion as in [1, 2, 16, 17] in order to take into account the potential nonlinearities of the aeroelastic system that can arise from *e.g.* geometric or localized nonlinearities. The plunge stiffness in Eq. 1(a) is written as $k_h h + k_{h3} h^3$. Similarly, $k_{\alpha 3}\alpha^3$ is introduced in Eq. 1(b). The nondimensional equations of motion then read

$$\tilde{\mathbf{q}}' = \mathbf{A}\tilde{\mathbf{q}} + \mathbf{b}, \tag{4}$$

with

$$\tilde{\mathbf{q}} = \begin{bmatrix} y \\ \alpha \\ \tilde{x} \\ y' \\ \alpha' \\ \tilde{x}' \end{bmatrix}, \mathbf{A} = \begin{bmatrix} 0_3 & Id_3 \\ -\mathbf{M}^{-1}\mathbf{K} & -\mathbf{M}^{-1}\mathbf{C} \end{bmatrix},$$

$$\mathbf{b} = \begin{bmatrix} 0 \\ 0 \\ 0 \\ -\mathbf{M}^{-1} \begin{bmatrix} \xi_h y^3 + \varepsilon\xi(y - \tilde{x} - \lambda\alpha)^3 \\ \xi_\alpha \alpha^3 + \varepsilon\xi\lambda(\tilde{x} - y + \lambda\alpha)^3 \\ \xi(\tilde{x} - y + \lambda\alpha)^3 \end{bmatrix} \end{bmatrix},$$

where $\xi_h = k_{h3}/(M\omega_\alpha^2)$, $\xi_\alpha = k_{\alpha 3}/(Mb^2\omega_\alpha^2)$ and $\xi = k_3/(m\omega_\alpha^2)$. Unless otherwise specified, ξ_h and ξ_α are set equal to 1, while ξ is left variable in order to control the nature of the bifurcation. Eigenvalues and eigenvectors of $\mathbf{A}$ are computed for $\tilde{U} = \tilde{U}_f$. The system being of dimension 6, they are denoted respectively $d_{1..6}$ and $\mathbf{V}_{1..6}$. Besides, the real and imaginary part of $d_{1..6}$ are denoted $\lambda_{1..6}$ and $\omega_{1..6}$ respectively. The Hopf bifurcation is characterized by a pair of complex eigenvalues crossing the imaginary axis. At criticality for $\tilde{U} = \tilde{U}_f$, these eigenvalues, denoted (d_1, d_2), have a zero real part. Their corresponding eigenvectors are denoted $\mathbf{V}_1$ and $\mathbf{V}_2$. Because it has been found that in our case $\mathbf{V}_1$ to $\mathbf{V}_6$ are complex, the following transformation matrix is introduced [11, 15],

$$\mathbf{T} = \begin{bmatrix} \mathrm{Re}(\mathbf{V}_1) & \mathrm{Im}(\mathbf{V}_1) & \mathrm{Re}(\mathbf{V}_3) & \mathrm{Im}(\mathbf{V}_3) & \mathrm{Re}(\mathbf{V}_5) & \mathrm{Im}(\mathbf{V}_5) \end{bmatrix}.$$

The first-order Jordan form of Eq. (2) is obtained by changing the linear basis with the transform $\tilde{\mathbf{q}} = \mathbf{T}\mathbf{y}$, and the dynamics for $\mathbf{y}$ writes

$$\mathbf{y}' = \mathbf{W}\mathbf{y} + \tilde{\mathbf{b}}, \tag{5}$$

where $\tilde{\mathbf{b}} = \mathbf{T}^{-1}\mathbf{b}$ and $\mathbf{W} = \mathbf{T}^{-1}\mathbf{A}\mathbf{T}$. The reduced-order model is then selected by vanishing y_3 to y_6 and thus keeping only the first two coordinates. For a system containing only cubic nonlinearity, this reduction is equivalent to the first-order center manifold of the system [11, 12, 18]. Thus the nonlinear system containing the leading-order nonlinearity controlling the Hopf bifurcation reads

$$\begin{bmatrix} y_1' \\ y_2' \end{bmatrix} = \begin{bmatrix} 0 & \omega_1 \\ -\omega_1 & 0 \end{bmatrix} \begin{bmatrix} y_1 \\ y_2 \end{bmatrix} + \begin{bmatrix} \tilde{b}_1 \\ \tilde{b}_2 \end{bmatrix}, \tag{6}$$

where $\tilde{b}_1$ and $\tilde{b}_2$ are polynomial function of y_1 and y_2. Now that the dynamical system is reduced to its local dynamics, a transformation into polar normal form of Eq. (6) is performed and yields to

$$r' = \lambda_\alpha(\tilde{U} - \tilde{U}_f)r + \rho r^3, \tag{7}$$

with $y_1 = r\cos(\omega_1)$, $y_2 = r\sin(\omega_1)$ and $\lambda_\alpha = \partial\lambda/\partial\tilde{U}$, where $\lambda = \lambda_1$ for any $\tilde{U}$. It has to be noticed that Eq. (7) is only valid for $\tilde{U}$ in a neighbourhood of $\tilde{U}_f$, because Eq. (6, 7) result from a local analysis at criticality. The validity of this neigbourhood will be discussed in the next section. Eventually,

$$\rho = (1/8)(3a_{30} + a_{12} + b_{21} + 3b_{03}), \tag{8}$$

where a_{30} and a_{12} are respectively the polynomial coefficients of y_1^3 and $y_1y_2^2$ of $\tilde{b}_1$, similarly, b_{03} and b_{21} are respectively the polynomial coefficients of y_2^3 and $y_1^2y_2$ of $\tilde{b}_2$.

The non-trivial solution of Eq. (7) is equal to $\sqrt{-\lambda_\alpha(\tilde{U} - \tilde{U}_f)/\rho}$, thus if $\rho > 0$, this solution is valid for $\tilde{U} < \tilde{U}_f$ and the bifurcation is subcritical. Otherwise, if $\rho < 0$, the non-trivial solution of Eq. (7) is valid for $\tilde{U} > \tilde{U}_f$ and the bifurcation is supercritical. The value of ξ for which $\rho = 0$ (denoted ξ_c) is a function of ξ_α and ξ_h, and can directly be derived from Eq. (8). Because the analytical expression of $\mathbf{T}$ is particularly tedious, the expression of ξ_c is found numerically by using the parameters from table 1 and yields to :

$$\xi_c = 0.0116\xi_h + 0.0966\xi_\alpha. \tag{9}$$

If $\xi > \xi_c$, the instability is supercritical and if $\xi < \xi_c$, the instability is subcritical. The nonlinearity of the NLTVA is thus able to cancel the subcriticality of the bifurcation. The validation of the analytical procedure described above as well as the behaviour of the system in the post-critical regime is investigated in the next section.

Post critical regime

The analytical procedure described above is compared with numerical solution obtained by a continuation technique, using a pseudo-arclength method implemented in the software AUTO [19]. Direct time integration of the system Eq.(4) is also performed using the solver *ode45* from Matlab, which implements a variable step size fourth-order Runge-Kutta scheme.

First of all, the bifurcation diagram for the airfoil without NLTVA (*i.e.* with $\varepsilon = 0$) is shown in Fig. 4(a) and (b). The analytical solution is very close to the numerical solution, which is very promising for the analytical procedure.

Nevertheless, because the analytical method is devoted to local analysis, for $\tilde{U}$ significantly larger than $\tilde{U}_f$ the analytical solution deviates from the numerical solution.

The case with a LTVA (*i.e.* $\xi = 0$) is shown in Fig. 4(c) and (d). Unlike the case without NLTVA, the Hopf bifurcation is here subcritical. Hence a detrimental effect of having repelled the flutter velocity is to shift the originally supercritical Hopf bifurcation to a subcritical one. The most salient disadvantage of subcriticality lies in the appearance of a jump phenomenon at the flutter velocity, when increasing (and decreasing) the flow speed. In this example, when $\tilde{U}$ is slightly larger than $\tilde{U}_f$, the amplitude of pitch motion varies suddenly from 0 to 15 degrees, which may cause serious damage to the structure.

If the NLTVA is tuned such as $\xi = \xi_c = 0.1085$, then $\rho = 0$ and the Hopf bifurcation is thus supercritical. This case is represented in Fig. 4(e) and (f). As a consequence, the nonlinearity of the NLTVA has canceled the subcriticality, and so the *jump*, brought by the LTVA. It is also shown in Fig. 4(e) and (f) that the analytical solution is valid for a very narrow neighborhood of $\tilde{U}_f$. Indeed the expression of the analytical solution is a function of $\sqrt{1/\rho}$, thus for $\rho \simeq 0$ the analytical expression diverges. Eventually, the LCO amplitude has been reduced by the NLTVA. For example at $\tilde{U} = 1.4$, the LCO amplitude on pitch has been decreased by 26.5% compared to the case without NLTVA. Nevertheless, at the same time, the LCO amplitude on plunge has been increased by 90.8 %. Even if this increase seems large, it is remarked that the more inconvenient LCO are those on the pitch mode, because this is the most energetic mode of the system in the post-critical regime and even after an increase of 90.8 % the LCO amplitude on plunge remains small (7 % of the semi-chord).

CONCLUSION

In this work, the influence of an NLTVA on the airfoil flutter instability has been investigated. An analytical procedure as well as numerical continuation have been conducted. The presence of the NLTVA has shown three important effects : the flutter velocity has been repelled to 34.5% the flutter velocity with no NLTVA, the LCO amplitude on pitch has been decreased by 26.5 % and the subcriticality caused by the linear part of the NLTVA has been canceled by its nonlinear part. Further studies

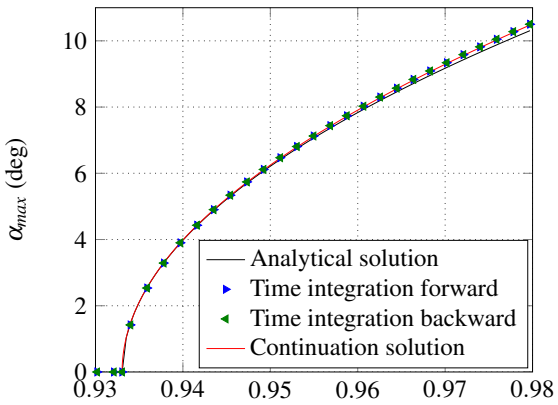

(a) $\tilde{U}$

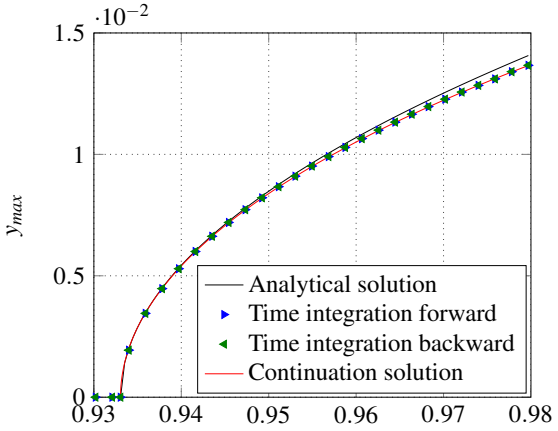

(b) $\tilde{U}$

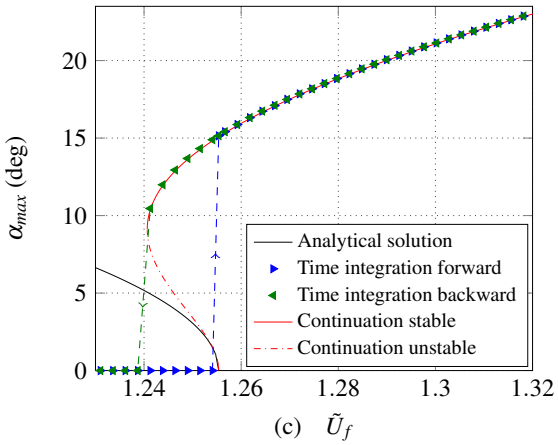

(c) $\tilde{U}_f$

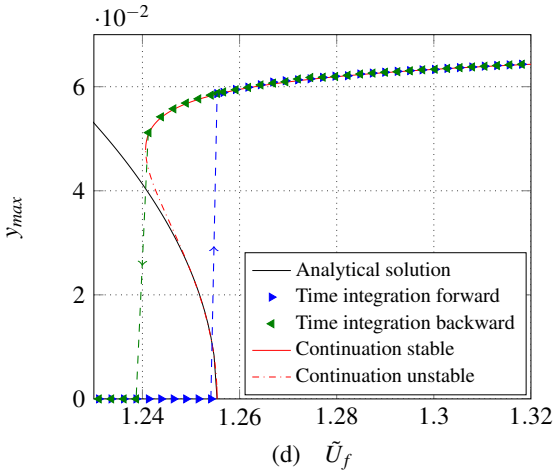

(d) $\tilde{U}_f$

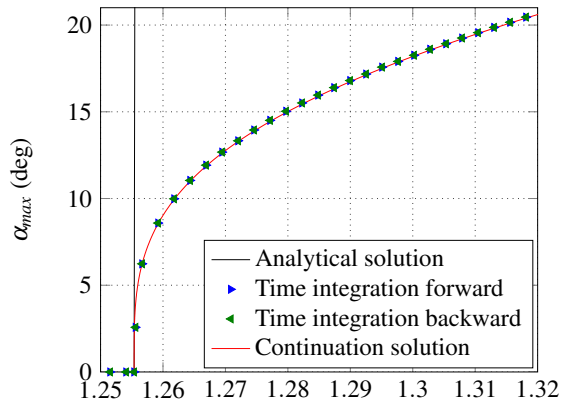

(e) $\tilde{U}_f$

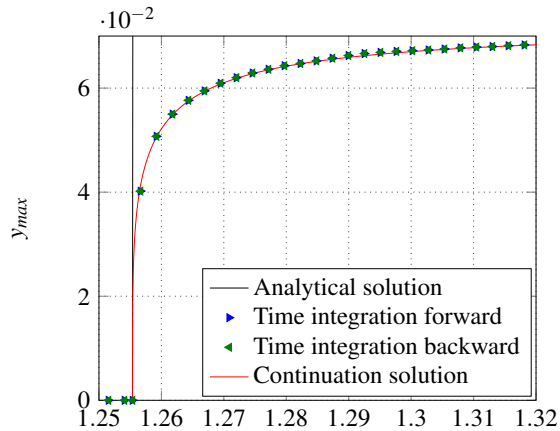

(f) $\tilde{U}_f$

FIGURE 4: Comparison between analytical, time integration and continuation solution of the system Eq. (4). (a) and (b) correspond to the system without NLTVA, (c) and (d) with a LTVA, (e) and (f) with an NLTVA and $\xi = \xi_c = 0.1085$.

could investigate the effectiveness of the NLTVA with other type of structural nonlinearities, such as softening nonlinearity, together with a more realistic aerodynamic model including nonlinearities developing at large amplitude motion.

ACKNOWLEDGMENT

We thanks Direction Générale de l'Armement (DGA) for a financial support to this work.

REFERENCES

[1] Lee, Y. S., Vakakis, A., Bergman, L., McFarland, D. M., and Kerschen, G., 2007. "Suppressing aeroelastic instability using broadband passive targeted energy transfers, part 1: theory". *AIAA journal,* ***45***(3), pp. 693–711.

[2] Lee, Y. S., Kerschen, G., McFarland, D. M., Hill, W. J., Nichkawde, C., Strganac, T. W., Bergman, L. A., and Vakakis, A. F., 2007. "Suppressing aeroelastic instability using broadband passive targeted energy transfers, part 2: experiments". *AIAA journal,* ***45***(10), pp. 2391–2400.

[3] Viguié, R., and Kerschen, G., 2009. "Nonlinear vibration absorber coupled to a nonlinear primary system: a tuning methodology". *Journal of Sound and Vibration,* ***326***(3), pp. 780–793.

[4] Habib, G., Detroux, T., Viguié, R., and Kerschen, G., 2015. "Nonlinear generalization of Den Hartog's equal-peak method". *Mechanical Systems and Signal Processing,* ***52***, pp. 17–28.

[5] Den Hartog, J. P., 1934. *Mechanical vibrations*. McGraw-Hill Book Company, Inc.

[6] Asami, T., Nishihara, O., and Baz, A. M., 2002. "Analytical solutions to H_∞ and H_2 optimization of dynamic vibration absorbers attached to damped linear systems". *Journal of vibration and acoustics,* ***124***(2), pp. 284–295.

[7] Krenk, S., and Høgsberg, J., 2014. "Tuned mass absorber on a flexible structure". *Journal of Sound and Vibration,* ***333***(6), pp. 1577–1595.

[8] Zilletti, M., Elliott, S. J., and Rustighi, E., 2012. "Optimisation of dynamic vibration absorbers to minimise kinetic energy and maximise internal power dissipation". *Journal of sound and Vibration,* ***331***(18), pp. 4093–4100.

[9] Habib, G., Detroux, T., and Kerschen, G., 2014. "Nonlinear generalization of den hartog's equal peak method for nonlinear primary systems". In Proceedings of the International Conference on Structural Nonlinear Dynamics and Diagnosis.

[10] Dowell, E. H., 1994. *A Modern Course in Aeroelasticity*. Kluwer Academic.

[11] Kuznetsov, Y. A., 2013. *Elements of applied bifurcation theory*, Vol. 112. Springer Science & Business Media.

[12] Guckenheimer, J., and Holmes, P., 2013. *Nonlinear oscillations, dynamical systems, and bifurcations of vector fields*, Vol. 42. Springer Science & Business Media.

[13] Manneville, P., 1995. "Dissipative structures and weak turbulence". *ChaosThe Interplay Between Stochastic and Deterministic Behaviour*, pp. 257–272.

[14] Iooss, G., and Adelmeyer, M., 1998. *Topics in bifurcation theory and applications*, Vol. 3. World Scientific.

[15] Habib, G., and Kerschen, G., 2015. "Suppression of limit cycle oscillations using the nonlinear tuned vibration absorber". In Proceedings of the Royal Society of London A: Mathematical, Physical and Engineering Sciences, Vol. 471, The Royal Society, p. 20140976.

[16] Lee, B., Jiang, L., and Wong, Y., 1998. "Flutter of an airfoil with a cubic nonlinear restoring force".

[17] Pettit, C. L., and Beran, P. S., 2003. "Effects of parametric uncertainty on airfoil limit cycle oscillation". *Journal of Aircraft,* ***40***(5), pp. 1004–1006.

[18] Gai, G., and Timme, S., 2015. "Nonlinear reduced-order modelling for limit-cycle oscillation analysis". *Nonlinear Dynamics*, pp. 1–19.

[19] Doedel, E. J., Paffenroth, R. C., Champneys, A. R., Fairgrieve, T. F., Kuznetsov, Y. A., Sandstede, B., and Wang, X., 2002. Auto 2000: Continuation and bifurcation software for ordinary differential equations. Tech. rep., Concordia University.

Appendix A: Coefficients of Eq. (3)

$$a_6 = r_\alpha^2 - x_\alpha^2,$$

$$a_5 = (\zeta_h + (1+\varepsilon)\zeta) r_\alpha^2 + (\nu x_\alpha + b r_\alpha^2)\tilde{U} + \zeta_\alpha - x_\alpha^2 \zeta + (2x_\alpha + \lambda)\varepsilon\lambda\zeta,$$

$$a_4 = (\Omega^2 + \zeta\zeta_h + (1+\varepsilon)\gamma + 1) r_\alpha^2 + (\beta\zeta_\alpha + (\nu x_\alpha + r_\alpha^2\beta)\zeta)\tilde{U} - (\beta x_\alpha + \nu)\tilde{U}^2 + (\zeta_h + (1+\varepsilon)\zeta)\zeta_\alpha + \varepsilon\lambda^2\zeta\zeta_h - \gamma x_\alpha^2 + (2x_\alpha + \lambda)\varepsilon\gamma\lambda,$$

$$a_3 = (\zeta\Omega^2 + (1+\gamma)\zeta_h + (1+\varepsilon)\zeta) r_\alpha^2 - (\nu\zeta_h + \beta x_\alpha\zeta + (1+\varepsilon)\nu\zeta)\tilde{U}^2 + (\beta\zeta\zeta_\alpha + \gamma\nu x_\alpha + r_\alpha^2\beta(1+\gamma))\tilde{U} + (\zeta\zeta_\alpha + \varepsilon\gamma\lambda^2)\zeta_h + (1+\varepsilon)\gamma\zeta_\alpha + (\zeta_\alpha + \varepsilon\lambda^2\zeta)\Omega^2,$$

$$a_2 = ((1+\gamma)\Omega^2 + \zeta\zeta_h + (1+\varepsilon)\gamma) r_\alpha^2 - (\nu\Omega^2 + \nu\zeta\zeta_h + \beta\gamma x_\alpha + (1+\varepsilon)\gamma\nu)\tilde{U}^2 + \beta(\gamma\zeta_\alpha + r_\alpha^2\zeta)\tilde{U} + (\zeta\zeta_\alpha + \varepsilon\gamma\lambda^2)\Omega^2 + \gamma\zeta_\alpha\zeta_h,$$

$$a_1 = (\zeta\Omega^2 + \gamma\zeta_h) r_\alpha^2 - \nu(\zeta\Omega^2 + \gamma\zeta_h)\tilde{U}^2 + \beta\gamma r_\alpha^2\tilde{U} + \gamma\zeta_\alpha\Omega^2,$$

$$a_0 = (r_\alpha^2 - \nu\tilde{U}^2)\gamma\Omega^2.$$